2008 IEEE International Conference on
Robotics and Automation
Pasadena, CA, USA, May 19-23, 2008

A new method for the estimation of position accuracy in parallel manipulators with joint clearances by screw theory

Antonio Frisoli*, Massimiliano Solazzi*, Massimo Bergamasco*

Abstract— **This paper presents a novel method based on screw theory for the analysis of positioning accuracy in parallel manipulators with joint clearances. A general method is introduced, and a new analytical procedure is formulated which allows to determine analytically a sub-optimal estimation of the worst case condition for positioning accuracy. Moreover this procedure can determine exactly the worst-case angular accuracy in translating fully-parallel manipulators under the influence of joint clearances. The relevance of the method is demonstrated by two application examples, that clearly demonstrate how kinematic properties, such as kinematic isotropy, are strictly related to position accuracy in mechanisms with joint clearances.**

I. Introduction

Joint clearance in mechanisms, due to dimension tolerances of kinematic pairs, may cause unavoidable positioning errors of the end-effector, with a consequent overall loss of accuracy of the system. Different factors, such as manufacturing tolerances or also a poor kinematic design, may lead to the detriment of positioning accuracy; it appears so evident the importance to develop reliable analytical tools that allow to simulate and predict the effects of clearances, since the earlier stages of design of a new mechanism.

Previous works have already investigated the effect of joint clearances on mechanism acccuracy, but however with several limitations, since most of them are limited to single-loop or planar mechanisms and do not fully address the design issues of more complex spatial parallel manipulators. In Tsai et al. [1] a screw theory method is used for determining the transmission performance of closed-loop linkages, but the method is applied to planar mechanisms only, while in Ting et al. [2] the analysis is limited to single-loop linkages. In Bamberger et al. [3], the authors examine the kinematic effects of large joint clearances in planar mechanisms. Other works rely on numerical approaches, such as interval analysis [4] or probabilistic methods [5], without proposing closed analytical solutions.

Unfortunately in parallel manipulators with several joints, the computation of the pose error with joint clearances is not an easy problem to solve. In Innocenti [6] a method is proposed for assessing the amount of positioning accuracy of a spatial robot under the application of a given load, but without providing a procedure for the estimation of the worst pose error, that normally requires the solution of a minimization problem. Recently, Venanzi et al. [7] presented an interesting general methodology both for the computation of positioning accuracy in spatial parallel manipulators and for the maximization of pose error functions. The approach is analytical and can lead to closed form solutions, based on the assumption of small displacements, but the analytical solution is limited only to the maximization with single components of the resultant end-effector motion handled separately.

With respect to previous research, in this paper we propose a new and original method, based on screw theory, which allows to compute the effect of clearances on the motion accuracy and the best/worst performance of a spatial manipulator under a generic pose error function, that can be expressed as a quadratic function of the end-effector displacement. The method makes use of a suboptimal analytical solution for the estimation of the worst case pose error function, that then allows to easily determine in a few numerical computation steps the worst case condition. Moreover it is shown that the presented approach represents the exact analytical solution for the determination of angular accuracy in an important class of parallel manipulators, the fully-parallel purely translational or rotational mechanisms. As a further important contribution of this paper, it is shown how the accuracy of a spatial parallel manipulator, influenced by the joint clearances, is strictly related to the kinematic isotropy of the current pose of the manipulator, measured through the condition number. To illustrate these concepts, three application examples are provided based on different configurations of translational fully parallel manipulators, that show how a poor kinematic design determines a higher accuracy error induced by joint clearances.

II. A general methodology for the determination of motion induced by clearances

The pose error of a mechanism induced by clearances can be easily estimated through the introduction of additional degrees of freedom (DOFs), representing the displacements in the kinematic pair caused by clearance. This is equivalent to remove all the constraints that the mechanical clearance make ineffective. If we consider for instance the case of a rotational joint, the effect of clearance can be modeled by the introduction of two rotations perpendicular to the revolute axis, and three translations, as it is shown in the detailed view of figure 1.

In most of the mechanisms, the magnitude of clearance in the joints is limited and its value is reasonably of a lower order of magnitude than the mechanism dimensions. Under

This work was partially funded under a research grant by the IP Presenccia and Strep Decision in Motion research project, funded by the European Commission.

* Authors are with the PERCRO Laboratory, Scuola Superiore Sant'Anna, Italy (http://www.percro.org). For communications, please contact a.frisoli@sssup.it.

the hypothesis of small displacements, several important assumptions can be drawn:

- the displacements at the end-effector, due to clearances in different joints, are independent of each other;
- the contributions of the clearances to the pose error of the end-effector, calculated given the tolerances in the pairs and according to the parallel kinematics, are composed as a linear summation to determine the resulting motion of the platform;
- the clearance analysis can be studied as a velocity analysis, using screw theory to define the infinitesimal displacements due to mechanical play: twists of zero and infinite pitch represent respectively rotations and translations;
- the contribution of each clearance to the overall motion of the coupler depends only on the pose of the mechanism.

This last consideration is particularly important, because it points out how the magnitude of clearance is highly influenced by the pose and so by the degree of kinematic isotropy of the mechanism.

A. A screw theory modeling of clearances

Under the hypothesis of small displacements, let us consider a generic parallel manipulator, such as the one shown in figure 2, whose leg is represented in figure 1.

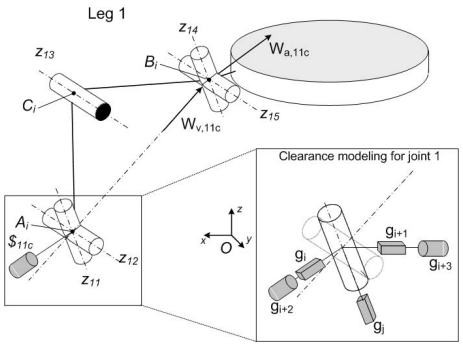

Fig. 1. A general scheme of a parallel manipulator with clearances

Assume that all the active DOFs are locked by the actuators (shown as darkened in figure 1), in such a way that the structure is statically determined and according to Grüber mobility equation [8] it has not any DOF; under the hypothesis of an isostatic spatial mechanism, a system of six linearly independent wrenches $\{\mathbf{W_{v,lm}}\}$, with pedex l indicating the leg number and m the wrench number, represents the active (due to the locked actuators) and passive constraints of the kinematics chains of the mechanism, as by [9]. For example in the manipulator of figure 2, the six constraint wrenches associated to each leg are shown on the kinematics, where the $\mathbf{W_{i1}}$ represent the actuation wrenches of zero pitch and the $\mathbf{W_{i2}}$ the passive constraint wrenches of infinite pitch.

When clearance effects are considered, an additional clearance-due DOF is equivalently introduced at the j-th joint

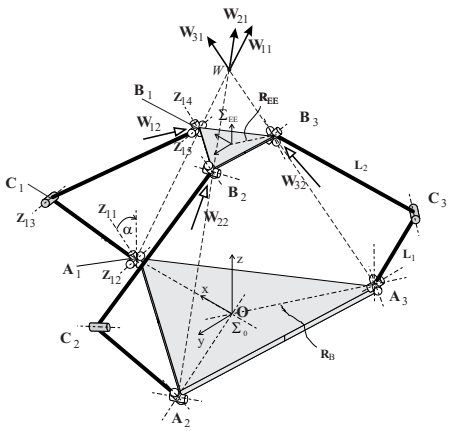

Fig. 2. The kinematics of the 3URU parallel manipulator. The manipulator is actuated on the third R joint of each leg.

of the i-th kinematic chain, as shown for example in the left part of figure 1, where a rotational joint $\$_{11c}$ (in gray) is added to the first rotational joint, to model a mechanical play orthogonal to the axis of the kinematic pair. In general, as shown in the right part of the same figure, up to $6-g$ clearance displacements can be associated to each kinematic pair with g dofs, and the kinematic chain correspondingly gains $6-g$ dof of mobility. Each clearance displacement can be associated to a corresponding twist $\$_{ijc}$ at the end-effector, where with the adopted notation i is the leg number, j and c respectively the joint and the clearance associated numbers.

Using the superimposition principle for the composition of small displacements, we will consider first the effect on the mobility of the system of a single clearance displacement $\$_{ijc}$ in leg i at joint j. For instance let us compute the effect of the screw $\$_{11c}$, representing the degree of freedom added to the first joint and modelling the associated mechanical clearance, represented in gray in figure 1, with the following expression

$$\mathbf{\$_{11c}} = \begin{pmatrix} \mathbf{w} \\ (\mathbf{A_i} - \mathbf{O}) \times \mathbf{w} \end{pmatrix} \quad \text{with} \quad \mathbf{w} = \frac{\mathbf{z_{11}} \times \mathbf{z_{12}}}{||\mathbf{z_{11}} \times \mathbf{z_{12}}||} \quad (1)$$

By writing down the differential kinematic law for leg i, the resultant generic motion of the end-effector $\mathbf{T_{ijc}}$ induced by the clearance $\mathbf{\$_{ijc}}$ can be expressed as:

$$\mathbf{T_{ijc}} = \sum_{k=1, k\neq n_a}^{n_j} (\delta\theta_{ik} \mathbf{\$_{ik}}) + g_{ijc} \mathbf{\$_{ijc}} \quad (2)$$

where $\delta\theta_{ik}$ are small displacements along the Lagrangian coordinates of the joints, except the actuated one n_a that is considered locked, g_{ijc} is the value of the additional clearance displacement and n_j the number of joints in the leg.

According to the dimension of the screw system expressed by equation (2), we can associate to each joint clearance $\$_{ijc}$,

a set of reciprocal wrenches denoted by $\mathbf{W_{ijc}}$, that fall into two main categories, let us call them of type α and type β.

Wrenches of type α, that we will denote as $\mathbf{W}_{\alpha,\mathbf{ijc}}$, are reciprocal to all the twists $\$_{ik}$ composing the leg i plus the additional clearance DoF $\$_{ijc}$, except for the locked actuated DoF $\$_{n_a}$. This set of wrenches is defined by the following equations, where $\otimes$ denotes the product of reciprocity between screws [10]:

$$\begin{cases} \mathbf{W}_{\alpha,\mathbf{ijc}} \otimes \$_{ijc} = 0 \\ \mathbf{W}_{\alpha,\mathbf{ijc}} \otimes \$_{ik} = 0 \qquad \text{for } \; k = 1..n_j, k \neq n_a \end{cases} \tag{3}$$

Analogously we can define the reciprocal wrenches of type β, that we will denote as $\mathbf{W}_{\beta,\mathbf{ijc}}$, as the wrenches reciprocal to all the twists $\$_{ik}$, but not to $\$_{ijc}$, as

$$\begin{cases} \mathbf{W}_{\beta,\mathbf{ijc}} \otimes \$_{ijc} \neq 0 \\ \mathbf{W}_{\beta,\mathbf{ijc}} \otimes \$_{ik} = 0 \qquad \text{for } \; k = 1..n_j, k \neq n_a \end{cases} \tag{4}$$

For example, the effect of the the degree of freedom added to the first joint and modeling the associated mechanical clearance (in gray), in the manipulator shown in figure 1, can be represented as a screw $\$_{11c}$.

In this example, the wrench system of type α reduces to one single wrench $\mathbf{W}_{\alpha,\mathbf{11c}}$. The wrench $\mathbf{W}_{\alpha,\mathbf{11c}}$ is a wrench of zero pitch, reciprocal to all $\$_{1k},, k = 1, 2, 4, 5$, except $\$_{13}$, and represents the constraint force exerted by the leg 1, directed along the line joining the two U joints. It can be expressed as:

$$\mathbf{W}_{\alpha,\mathbf{11c}} = \begin{pmatrix} \mathbf{v} \\ (\mathbf{A_i} - \mathbf{O}) \times \mathbf{v} \end{pmatrix} \tag{5}$$

with

$$\mathbf{v} = \frac{\mathbf{B_1} - \mathbf{A_1}}{||\mathbf{B_1} - \mathbf{A_1}||} \tag{6}$$

The wrench system of type β are composed of $\mathbf{W}_{\beta,\mathbf{11c}}$, a wrench of infinite pitch reciprocal to all $\$_{1k}, k = 1, 2, 4, 5$, but not to $\$_{11c}$, representing the action of a virtual actuator controlling the clearance DoF:

$$\mathbf{W}_{\beta,\mathbf{11c}} = \begin{pmatrix} 0 \\ \mathbf{w} \end{pmatrix} \tag{7}$$

According to (3) and (4), the virtual work done by the wrenches $\mathbf{W}_{\alpha,\mathbf{ijc}}$ and $\mathbf{W}_{\beta,\mathbf{ijc}}$ along the displacement $\mathbf{T_{ijc}}$ can be computed as:

$$\begin{cases} \mathbf{W}_{\alpha,\mathbf{ijc}} \otimes \mathbf{T_{ijc}} = 0 \\ \mathbf{W}_{\beta,\mathbf{ijc}} \otimes \mathbf{T_{ijc}} = g_{ijc} \left(\mathbf{W}_{\beta,\mathbf{ijc}} \otimes \$_{ijc} \right) \end{cases} \tag{8}$$

The work done by the constraint wrenches $\{\mathbf{W_{lm}}\}$ associated with the other legs $l \neq i$, along the displacement $\mathbf{T_{ijc}}$, is null too and so the following equation (9) holds:

$$\mathbf{W_{lm}} \otimes \mathbf{T_{ijc}} = 0 \qquad \text{with} \quad l \neq i \tag{9}$$

The wrenches $\mathbf{W}_{\alpha,\mathbf{ijc}}$, $\mathbf{W}_{\beta,\mathbf{ijc}}$ and $\mathbf{W_{lm}}$ (with $l \neq i$) define a system of 6 wrenches, that can be arranged in a matrix W:

$$W = \begin{pmatrix} \mathbf{W}_{\beta,\mathbf{ijc}} \mathbf{W}_{\alpha,\mathbf{ijc}} & \dots & \mathbf{W_{lm}} \end{pmatrix} \tag{10}$$

Equations (8) and (9) can be put in matricial form as:

$$W^T I^* \mathbf{T_{ijc}} = \begin{pmatrix} g_{ijc} \left(\mathbf{W}_{\beta,\mathbf{ijc}} \otimes \$_{ijc} \right) \\ 0 \\ \vdots \\ 0 \end{pmatrix} \tag{11}$$

with the matrix I^* composed of the 3×3 identity and zero matrices:

$$I^* = \begin{pmatrix} 0_3 & I_3 \\ I_3 & 0_3 \end{pmatrix} \tag{12}$$

Since I^* and W^T are always invertible, the contribution $\mathbf{T_{ijc}}$ of the clearance DoF can be obtained by inverting the relation (11) as:

$$\mathbf{T_{ijc}} = (W^T I^*)^{-1} \begin{pmatrix} g_{ijc} \left(\mathbf{W}_{\beta,\mathbf{ijc}} \otimes \$_{ijc} \right) \\ 0 \\ \vdots \\ 0 \end{pmatrix} = \hat{\mathbf{T}}_{\mathbf{ijc}} g_{ijc} \tag{13}$$

where $\hat{\mathbf{T}}_{\mathbf{ijc}}$ indicates the screw associated with the motion induced by the clearance with unitary clearance at joint $\$_{ijc}$.

Under the hypothesis of small displacements, we can compose linearly the overall pose errors of the end-effector $\$$ due to multiple clearances g_{lkc}, resulting in:

$$\$ = \sum_{(l=1,k=1,c=1)}^{(i=n_l,j=n_j,c=n_c)} \hat{\mathbf{T}}_{\mathbf{lkc}} g_{lkc} = T\mathbf{g} \tag{14}$$

where the columns of T are the single normalized contributes $\hat{\mathbf{T}}_{\mathbf{lkc}}$ of the clearance DoF as by (13) and the elements of $\mathbf{g}$ are the associated values of displacement:

$$T = \begin{pmatrix} \hat{\mathbf{T}}_{\mathbf{111}} & .. & \hat{\mathbf{T}}_{\mathbf{11n_c}} & .. & \hat{\mathbf{T}}_{\mathbf{1n_jn_c}} & .. & \hat{\mathbf{T}}_{\mathbf{n_{leg}n_jn_c}} \end{pmatrix}$$

$$\mathbf{g} = \begin{pmatrix} g_{111} \\ . \\ . \\ g_{11n_c} \\ \vdots \\ g_{1n_jn_c} \\ \vdots \\ g_{n_{leg}n_jn_c} \end{pmatrix} \tag{15}$$

III. An analytical procedures for determination of clearances in parallel systems

A. Clearance in rotational joints

We will restrict our analysis to the position accuracy of parallel manipulators with rotational joints only and joint clearances. The vector $\mathbf{g}$ in (15) is composed of the independent parameters g_i used for describing the clearance at the level of each joint. These clearance variables are

not independent, but are usually coupled by non-linear constraints, and in particular for a rotational joint depend on the actual mechanical design the joint. We will assume a modeling of clearance in a rotational joint that is valid for pairs implemented with ball bearings, which represents a common method of implementation. The scheme of figure 3 shows the composition of different clearance displacements in a ball bearing joint in the two cases of clearances on inner or outer ring.

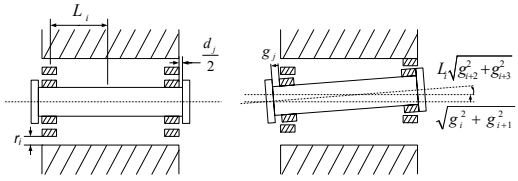

(a) Clearance between the housing and the outer ring

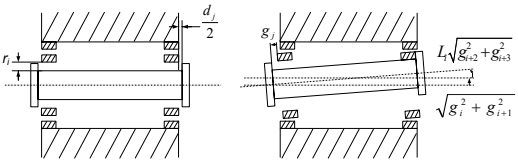

(b) Clearance between the pin and the inner ring

Fig. 3. Indication of clearances in a rotational joint

In particular, we will consider R joints characterized by the following two types of constraint, according to figure 3:

Clearance of type a.

The clearance motion of the pair is the combination of the linear displacement of the hinge, perpendicular to its axis, and a rotation along two axes perpendicular to the hinge axis. The possible range of motion is defined by a clearance model, described by a function C_a:

$$C_a(g_i, g_{i+1}, g_{i+2}, g_{i+3}) = g_i^2 + g_{i+1}^2 + L_i^2(g_{i+2}^2 + g_{i+3}^2) - r_i^2 \leq 0 \tag{16}$$

where L_i is the semilength of the rotational pair. The set of clearances g_i, g_{i+1} represents displacements, while g_{i+2}, g_{i+3} rotations of the joint axis, and can be equivalently represented with virtual prismatic and rotational joints as in figure 1.

The interpretation of this constraint can be given as in figure 3(a) in the case of radial clearance r_i between the housing and the outer ring, and in figure 3(b) where the same clearance r_i is between the pin and the inner ring. The resulting displacement $\sqrt{g_i^2 + g_{i+1}^2}$ and rotation $\sqrt{g_{i+2}^2 + g_{i+3}^2}$ can occur also in different planes; in figure 3 only coplanar displacements are shown for sake of a clearer visualization. We can normally simplify this constraint by adopting a set of homogeneous coordinates, converting rotations to displacements by multiplication with a reference length (in this case the semilength of the pair L_i), such that we get a new set of variables defined as $g'_{i+2} = L_i g_{i+2}$ and $g'_{i+3} = L_i g_{i+3}$. In the following we will assume that the function C_a can be cast in the form $\sum_{k=i}^{k=i+4} g_k^2 \leq r_i^2$ with this set of homogeneous coordinates, by omitting the apex for sake of simplicity.

Clearance of type b.

This constraint is characterized by a linear displacement along the hinge axis, as shown in figure 3 for the two cases.

$$C_b(g_j) = g_j^2 - d_j^2 \leq 0 \tag{17}$$

This clearance is controlled by the axial tolerances of mounting of the bearings, and is shown as an equivalent prismatic pair in figure 1.

B. Determination of maximum clearance

The problem of determining the maximum clearance in a manipulator can be analytically formulated as follows. Given a metrics matrix M, positive definite and symmetric, let us define the generic functional:

$$f = \$^T M \$ = \mathbf{g}^T T^T M T \mathbf{g} = \mathbf{g}^T A \mathbf{g} \tag{18}$$

Define also the set of the points g_i that verify the constraints of type a or b respectively according to the model assumed for each joint, as the ball $B \in \Re^n$ with

$$(g_{i,a}^2 + g_{i+1,a}^2) + (g_{i+2,a}^2 + g_{i+3,a}^2) \leq r_i^2 \quad \text{if } C_a(R_i) \leq 0 \tag{19}$$

$$g_{j,b}^2 \leq d_j^2 \quad \text{if } C_b(R_j) \leq 0 \tag{20}$$

It is easy to see from (19) and (20) that the points $\mathbf{g}$ are contained within the hypersphere B of $\Re^n$ with boundary ∂B and radius r:

$$r = \sqrt{\sum_i r_i^2 + \sum_j d_j^2} \tag{21}$$

The maximum clearance is the set of joint clearances displacement $\mathbf{g} \in B$ which maximize the functional f:

$$\max_{\mathbf{g} \in B} (\mathbf{g}^T A \mathbf{g}) \text{ with } C_k(g_i) \leq 0,\ k = a, b \tag{22}$$

The above formulation is quite general and includes all the main cases of clearance generated by rotational joints in parallel manipulators.

Lemma 1 (Properties of the solution of equation (22))**.** *The functional f in* (22) *has always a minimum for $\mathbf{g} = 0$ and reaches always its maximum evaluated in the ball B on the boundary ∂B.*

Proof. We can state two properties about equation (22):

1) The matrix A is semidefinite positive.
2) The gradient of f is always directed toward the boundary ∂B.

The first property derives easily from the definition of matrix A. Since M is positive definite, we have $\$ \cdot M \$ > 0$, and so from 18 we can easily derive $\mathbf{g} \cdot A\mathbf{g} \geq 0$, where the expression is zero for $\mathbf{g} \neq 0$, only if $\det(A) = 0$ and $\mathbf{g}$ is chosen in the kernel of A.

The second property can be also easily verified, since A is semidefinite positive:

$$\text{grad}(f) \cdot \mathbf{g} = \frac{\partial f}{\partial \mathbf{g}} \cdot \mathbf{g} = 2A\mathbf{g} \cdot \mathbf{g} \geq 0 \tag{23}$$

These two properties demonstrate lemma 1. □

By using lemma 1, we can formulate in a equivalent way the maximization clearance problem as:

$$\max_{g_i \in \partial B} (\mathbf{g}^T A \mathbf{g}) \text{ with } C_k(g_i) = 0|_{k=a,b,c} \tag{24}$$

The interpretation of this results is intuitive, meaning that in the condition of maximum displacement all the clearance pairs reach their limit position.

1) An efficient parametrization of the domain ∂B: We can easily find a suboptimal solution for this maximization problem.

Let us assume a parametrization of points on $\mathbf{g} \in \partial B$ as follows. If $C_a(R_i) = 0$, then the points $g_i, \ldots, g_{i+3}$ can be parameterized as a function of three new parameters $\theta_i, \theta_{i+1}, \phi_i$:

$$\mathbf{g_{i,a}} = \begin{bmatrix} g_i \\ g_{i+1} \\ g_{i+2} \\ g_{i+3} \end{bmatrix} = r_i \begin{bmatrix} \cos(\theta_i)\cos\phi_i \\ \sin(\theta_i)\cos\phi_i \\ \cos(\theta_{i+1})\sin\phi_i \\ \sin(\theta_{i+1})\sin\phi_i \end{bmatrix} \tag{25}$$

It is straightforward to verify that points given by (25) satisfy equation (19). The cosine and sine of angle ϕ_i are the percentage of clearance that is converted in either displacement or rotation of the hinge axis of the associated rotational pair.

If $C_b(g_j) = 0$, we will consider the two different conditions of either $g_j = +d_j$ or $g_j = -d_j$, with g_j a constant value, so that no parametrization is needed in this case.

We will assume so for the description of our search domain ∂B, a reduced set of coordinates composed of the angles θ_i and ϕ_i introduced in (25). It is easy to show that, due to the properties of derivatives of sines, cosines and constant functions, this parametrization has the following properties:

$$\begin{cases} \frac{\partial \mathbf{g_{i,a}}}{\partial \theta_j} \cdot \mathbf{g_{i,a}} = 0 \quad \text{with } j = i, i+1 \\ \frac{\partial \mathbf{g_{i,a}}}{\partial \phi_i} \cdot \mathbf{g_{i,a}} = 0 \end{cases} \tag{26}$$

2) The optimal solution of the maximization problem over ∂B: Since A is a symmetric matrix with real eigenvalues λ_i and orthogonal eigenvectors $\mathbf{v_i}$ and our functional f is a quadratic function of the matrix A constrained on the boundary ∂B of an hypersphere, it is straightforward to determine its maximum overall ∂B.

Lemma 2 (Maximization of f over ∂B)**.** *The clearance vector that maximizes the functional f on the hypersphere ∂B is $\mathbf{g_{opt}} = r\mathbf{v_{max}}$, with $\mathbf{v_{max}}$ the eigenvector associated to the maximum eigenvalue of A and r given by* (21)*.*

Proof. We can assume as basis of $\Re^n$ the eigenvectors $\mathbf{v_i}$ of A and expressing the clearance vector $\mathbf{g}$ as a function of coordinates α_i such that $\mathbf{g} = \sum_i \alpha_i \mathbf{v_i}$. Since $A\mathbf{v_i} = \lambda_i \mathbf{v_i}$, it is easy to see how the expression of the functional $\mathbf{g}^T A\mathbf{g}$ becomes $f = \sum_i \alpha_i^2 \lambda_i$. We can maximize f under the constraint of $\mathbf{g} \in \partial B$, that is $\sum_i \alpha_i^2 = r^2$. This is equivalent to the maximization of a function $g = f - \gamma(\sum_i \alpha_i^2 - r^2)$, with γ a Lagrange multiplier. By computing the partial derivatives of g and setting them equal to zero, we find

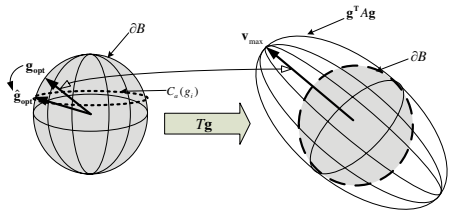

Fig. 4. Geometrical interpretation of the mapping of the hypersphere ∂B by $T\mathbf{g}$

$$\begin{cases} \frac{\partial g}{\partial \alpha_i} = 2\alpha_i(\lambda_i - \gamma) = 0 \quad \rightarrow \gamma = \lambda_k, \alpha_j = 0 \text{ for } \forall j \neq k \\ \frac{\partial g}{\partial \gamma} = \sum_i \alpha_i^2 - r^2 = 0 \end{cases} \tag{27}$$

The above conditions mean that the maximum is reached when the clearance vector is aligned with one of the eigenvector and it is easy to see how the optimal solution is obtained for the eigenvector $\mathbf{v_{max}}$ associated to the maximum eigenvalue, so that $\mathbf{g_{opt}} = r\mathbf{v_{max}}$. This is a direct consequence of the quadratic mapping of the hypersphere of radius r into an hyperellipsoid with semiaxes given by the eigenvalues, as shown in figure 4.

□

However the optimal clearance vector, obtained as by lemma 2 will not necessarily satisfy the clearance constraints (16) and (17). We will show now a procedure to obtain a suboptimal value $\widehat{\mathbf{g}}_{\mathbf{opt}}$ once the value of $\mathbf{g_{opt}}$ is known.

3) The suboptimal solution of the maximization problem over ∂B: We will choose as an approximation of the optimal solution, the vector of clearances on ∂B, satisfying the clearance constraints, that is the closest one to the optimal value $\mathbf{g_{opt}}$, according to the two following norms:

$$\begin{cases} 1.\ \text{Maximum projection: } o_1 = \mathbf{g} \cdot \mathbf{g_{opt}} \\ 2.\ \text{Minimum distance: } o_2 = (\mathbf{g} - \mathbf{g_{opt}})^T \cdot (\mathbf{g} - \mathbf{g_{opt}}) \end{cases} \tag{28}$$

Under some cases, it can be also demonstrated that this projection of the optimal point $\mathbf{g_{opt}}$ in the constraint space is also the optimal point in the constraint space. However it is a good starting point for a maximization gradient-based numeric algorithm, that will converge to the absolute maximum in a limited number of iteration steps.

Theorem 1 (Suboptimal solution)**.** *The best approximation under norms o_1 and o_2 of $\mathbf{g_{opt}}$, is given by the vector $\widehat{\mathbf{g}}_{\mathbf{opt}}$, whose expression is given as follows. Denote the optimal vector as $\mathbf{v} = \mathbf{g_{opt}}$. Then, using the parametrization on ∂B for constraints of type a:*

Constraints of type a.

Choose

$$\begin{cases} \theta_i = \textit{atan2}(v_{i+1}, v_i) \\ \theta_{i+1} = \textit{atan2}(v_{i+3}, v_{i+2}) \\ \phi_i = \textit{atan2}(\sqrt{v_{i+3}^2 + v_{i+2}^2}, \sqrt{v_{i+1}^2 + v_i^2}) \end{cases} \quad (29)$$

Constraints of type b.
Choose $g_j = \operatorname{sgn}(v_j) d_j$

Proof. The demonstration can be carried out by computing the partial derivatives of norms o_1 and o_2 and setting them equal to zero, according to the constraint a. Let us consider before the norm $o_1 = \mathbf{g} \cdot \mathbf{v}$. In this case, with the adopted parametrization, it is easy to show that for constraints of type a:

$$\frac{\partial o_1}{\partial \theta_i} = \frac{\partial \mathbf{g}}{\partial \theta_i} \cdot \mathbf{v} = r_i \cos(\phi_i)[-\sin(\theta_i) v_i + \cos(\theta_i) v_{i+1}] = 0 \quad (30)$$

$$\frac{\partial o_1}{\partial \theta_{i+1}} = r_i \sin(\phi_i)[-\sin(\theta_i) v_{i+2} + \cos(\theta_i) v_{i+3}] = 0 \quad (31)$$

$$\frac{\partial o_1}{\partial \phi_i} = \frac{\partial \mathbf{g}}{\partial \phi_i} \cdot \mathbf{v} = r_i[-\sin(\phi_i)(\cos(\theta_i) v_i + \sin(\theta_i) v_{i+1}) + \cos(\phi_i)(\cos(\theta_{i+1}) v_{i+2} + \sin(\theta_{i+1}) v_{i+3})] = 0 \quad (32)$$

From (30) and (31) we obtain the first two conditions of equation (29), and substituting them in (32), we easily obtain the last condition of (29).

For a constraint of type b, since we are assuming that g_j is constant, we should only decide the sign of g_j, and we assume it in the same direction of the maximum eigenvalue to maximize the projection. In this way we guarantee that the contribution of this projection term is always positive (like the previous ones) and better than the opposite choice of the sign $-\operatorname{sgn}(v_j)$:

$$g_j v_j = \operatorname{sgn}(v_j) d_j v_j = d_j \frac{v_j^2}{|v_j|} > -\operatorname{sgn}(v_j) d_j v_j \quad (33)$$

Due to property (26), we have that the partial derivatives of o_1 and o_2 with constraints of type a are equal, and so the above conditions satisfy also the minimization of norm o_2. For the choice of the sign of a constraint of type b, again we have that this represents the best choice of sign for minimizing the norm o_2:

$$(g_j - v_j)^2 = (\operatorname{sgn}(v_j) d_j - v_j)^2 < (-\operatorname{sgn}(v_j) d_j - v_j)^2 \quad (34)$$

□

C. The optimal solution for the clearance problem

Once we have found the expression for the suboptimal estimate $\widehat{\mathbf{g}}_{opt}$, we can easily find by means of a numeric procedure the optimal solution by a gradient descent method, using as starting guess point the obtained estimate. The process will converge to an absolute maximum, and not to a relative one, because a starting point in the neighborhood of the absolute maximum has been chosen, and the gradient of the functional f

$$\operatorname{grad} f = 2 \frac{\partial \mathbf{g}}{\partial \boldsymbol{\theta}} \cdot A\mathbf{g} \quad (35)$$

is continuous over the domain.

There are some special cases, for which the gradient expression (35) is null for the subotimal clearance vector estimate, and so the suboptimal solution represents also the optimal solution. It can be shown that such special cases are normally represented by mechanisms with 3dof and full-cycle mobility, such as planar kinematics, purely rotational or translational parallel mechanisms. This will be demonstrated for the case of a translational parallel mechanisms in the next section.

IV. Applications

This section presents application examples of the above method for the determination of angular or translational clearance in parallel manipulators. Two different configurations of a symmetrical parallel manipulator with pure translational motion [11], [12] are considered. Both clearances and condition numbers for different poses of the manipulator over the workspace are computed and their relation is analyzed. For the first device both angular and translational clearance is calculated.

A. A device for the stimulation of the fingerpad

Figure 2 shows the kinematics of a 3 DOFs haptic interface for the stimulation of the fingerpad, consisting of a 3URU parallel manipulator, with the actuation on the third joint. Each leg can apply to the end-effector a constraint wrench $\mathbf{W_{i1}}$ of infinite pitch, and an actuation wrench $\mathbf{W_{i2}}$ of zero pitch.

The kinematic dimensions of the mechanism under system are reported in table I according to the symbols shown in figure 2.

l_1 (mm)	l_2 (mm)	R_{EE} (mm)	R_B (mm)	α_0 (°)
17	17	33	47	36

TABLE I
DATA RELATIVE TO THE KINEMATICS SHOWN IN FIGURE 2

Each leg is composed of five rotational joints J_i, with $i = 1, 2 \ldots, 5$. We are now interested in determining the maximum angular displacement due to joint clearances. For this mechanism, the angular clearance at the end-effector is a relevant parameter, because it characterizes the extent to which the ideal kinematic behavior of the purely translational mechanism differs from the real one. In order to find the maximum angular clearance of the mechanism, we will consider a metrics defined by a matrix M

$$M = \begin{pmatrix} I_3 & 0_3 \\ 0_3 & 0_3 \end{pmatrix} \quad (36)$$

corresponding to the maximization of the angular displacement $\boldsymbol{\omega}^T \boldsymbol{\omega}$.

It can be shown in this case, how the clearances equivalent to prismatic joints, such as g_i, g_{i+1}, g_j in figure 1 for each rotational joint, produce only a translational motion and

so does not contribute to the overall angular clearance of the mechanism. This allows us to simplify the analysis by assuming a null value for the clearance parameter $\phi_i = 0$ in (25). In this case the dimension of the vector $\mathbf{g_{j,a}}$ becomes a 2×1 vector composed of the last two non null components of (25). In this hypothesis, it can be demonstrated that the clearance contributions introduced by each rotational joint, for small displacements, are for each leg only a screw of zero pitch, corresponding to an instantaneous rotation of the coupler.

Moreover in this class of mechanisms, it can be easily demonstrated (the demonstration is here omitted for sake of brevity), that due to this property, the subotimal solution $\widehat{\mathbf{g}}_{\mathbf{opt}}$ is also the optimal one, so the maximum angular pose error can be determined directly in one single computation step according to (29). We have assumed for each joint a maximum rotational clearance as reported in table II, derived from the tolerances of the mechanical design of the kinematic pair.

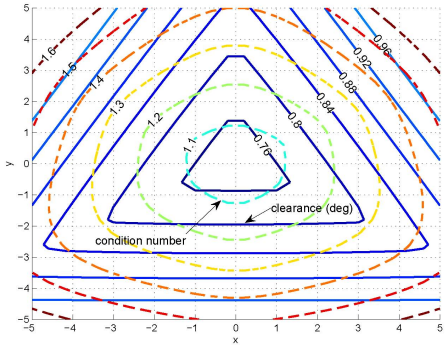

Fig. 5. A contour plot of condition number and clearance (degrees) of the first 3URU manipulator.

J1 (rad)	J2 (rad)	J3 (rad)	J4 (rad)	J5 (rad)
0.002	0.0011	0.0011	0.0011	0.002

TABLE II

ANGULAR PLAY OF THE LEG JOINTS OF THE KINEMATICS IN FIGURE 2

Once the maximum angular pose error was found, the condition number of the mechanism was computed in the same configuration, and this procedure was iterated for different displacements of the coupler in the horizontal plane. This allows to analyze the relation between the joint clearance and the resulting angular accuracy at the end-effector in relation with the kinematic configuration assumed by the manipulator, expressed as a function of the condition number. Figure 5 shows a contour plot of the condition number computed for the matrix of the constraint wrenches to rotations and the maximum allowed rotational clearance, for motions of the platform in the X-Y plane. The best performance of accuracy agrees with the best condition number, in the centre of the plane. It is interesting to notice how the degradation of clearance is reached when the condition number decreases. Both the condition number and the clearance are not affected by displacement along the z axis for $x = 0, y = 0$, due to the special adopted disposition of R joints in the leg.

B. Determination of the maximum translational clearance

The method is now applied to the kinematics of subsection IV-A in order to calculate the maximum translational clearance at the end effector. Then we will consider a metrics defined by a different matrix M

$$M = \begin{pmatrix} 0_3 & 0_3 \\ 0_3 & I_3 \end{pmatrix} \tag{37}$$

corresponding to the maximization of the translational displacement $\boldsymbol{x}^T\boldsymbol{x}$.

In this case every kinds of joint displacements can affect the accuracy at the end effector. The joint clearances $\mathbf{g_{i,a}}$ are parametrized according to equation 25, while the clearance g_j can assume values between $-d_j$ and d_j. The characteristic dimensions r_i, L_i and d_j of the joints (see figure 3) are shown in table III

	J1	J2	J3	J4	J5
radial play r_i (mm)	0.01	0.01	0.01	0.01	0.01
semilength L_i (mm)	5	9	9	9	5
axial play d_j (mm)	0.015	0.015	0.015	0.015	0.015

TABLE III

MECHANICAL TOLERANCES AND DIMENSIONS OF THE JOINTS OF EACH LEG OF THE KINEMATICS SHOWN IN FIGURE 2

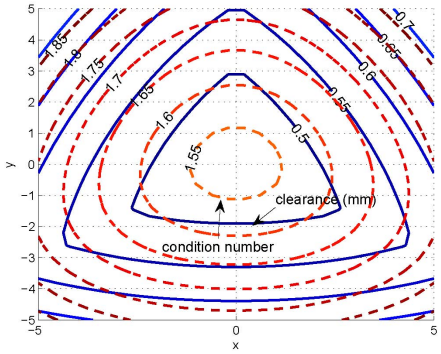

Fig. 6. A contour plot of condition number and translational clearance expressed in mm for the first 3URU manipulator.

Unlike the previous examples, in order to find the optimal solution $\mathbf{g_{opt}}$ is necessary to apply a gradient descent method, using the estimate $\widehat{\mathbf{g}}_{\mathbf{opt}}$ as starting guess point. The contour plot of figure 6 shows the relation between the condition number of the matrix of the actuation wrenches $\mathbf{W_{i0}}$ and the maximum allowed translational clearance. Figure 7(a) shows the number of iterations necessary to the gradient descent method to converge to a solution in different positions of the X-Y plane, while figure 7(b) is a plot of the first-order optimality.

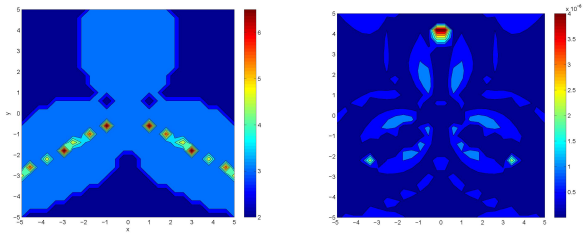

(a) N. of iterations (b) 1^{st} order optimality

Fig. 7. Convergence of the gradient descent method

C. A sensor cell for force measurement

Our second application example is a sensor cell composed of three monoaxial force sensors in order to measure a generic force in the space, whose kinematic is shown in figure 8(b).

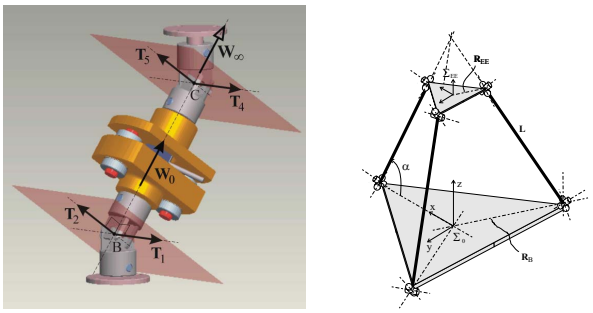

(a) The cell leg (b) The cell kinematics

Fig. 8. The sensor cell

Even if the kinematics is very similar to the example above, it presents different orientation of the R pairs; it has three UPU legs, where the sensor is mounted in the prismatic pair to measure the longitudinal force applied on the leg (figure 8(a)). The mechanism has the dimensions reported in table IV. In this example, for constructive reasons, all joints clearance are assumed equal to 0.004 rad.

l (mm)	R_{EE} (mm)	R_B (mm)	θ_0 (°)
105	39.6	129.8	59.2

TABLE IV
DATA OF THE MECHANISM SHOWN IN FIGURE 9

Also in this case, by applying our method we can determine the exact maximum angular pose error. Figure 9 shows the condition number and clearance as a function of z axis, i.e. the distance between the upper platform and the base. The minimum error is reached when also the minimum condition number is achieved, with a strict relationship between these two parameters. In this case, due to the different arrangement of the joints, it is possible to observe also a degradation of the performance over z. In both the two cases a design that takes into account the kinematic isotropy of the mechanism can also guarantee a higher accuracy of the mechanism, independently of the mechanical tolerances in the joints.

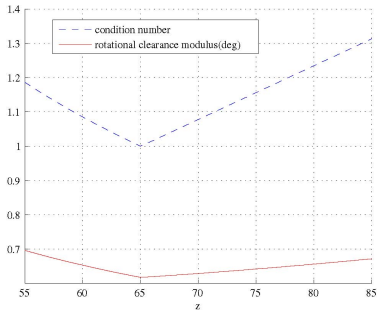

Fig. 9. A contour plot of condition number and clearance expressed in degrees for the cell sensor

V. CONCLUSIONS

This paper has presented a novel method for the determination of clearances in parallel manipulators, based on screw theory. The method is general, and allows to find a suboptimal estimation of the positioning accuracy under the influence of joint clearances. The method can tackle with an arbitrary pose error function based on a quadratic function of the displacement. For fully-translational parallel manipulators, and other classes, such as other full-cycle mobility parallel mechanisms, the method allows also to have a precise estimation of maximum displacement at the end-effector under the action of joint clearances. The relevance of such a result has been shown with three application examples, showing the relationship between kinematic condition number and positioning performance under joint clearances.

REFERENCES

[1] M.J. Tsai and T.H. Lai. Kinematic sensitivity analysis of linkage with joint clearance based on transmission quality. *Mechanism and Machine Theory*, 39(11):1189–1206, 2004.

[2] K.L. Ting, J. Zhu, and D. Watkins. The effects of joint clearance on position and orientation deviation of linkages and manipulators. *Mechanism and Machine Theory*, 35(3):391–401, 2000.

[3] H. Bamberger, M. Shoham, and A. Wolf. Kinematics of micro planar parallel robot comprising large joint clearances. *Advances in Robot Kinematics*, pages 75–84, 2006.

[4] Weidong Wu and S. S. Rao. Interval Approach for the Modeling of Tolerances and Clearances in Mechanism Analysis. *Journal of Mechanical Design*, 126:581, 2004.

[5] RE Garrett and AS Hall. Effect of Tolerance and Clearance in Linkage Design. *ASME Journal of Engineering for Industry*, 91(1):198–202, 1969.

[6] C. Innocenti. Kinematic clearance sensitivity analysis of spatial structures with revolute joints. *Journal of Mechanical Design(Transactions of the ASME)*, 124(1):52–57, 2002.

[7] S. Venanzi and V. Parenti-Castelli. A New Technique for Clearance Influence Analysis in Spatial Mechanisms. *Journal of Mechanical Design*, 127:446, 2005.

[8] J.M.R. Martínez and B. Ravani. On Mobility Analysis of Linkages Using Group Theory. *Journal of Mechanical Design*, 125:70, 2003.

[9] S.A. Joshi and L.W. Tsai. Jacobian Analysis of Limited-DOF Parallel Manipulators. *Journal of Mechanical Design*, 124:254, 2002.

[10] J. Gallardo, J. M. Rico, A. Frisoli, D. Checcacci, and M. Bergamasco. Dynamics of parallel manipulators by means of screw theory. *Mechanisms and Machine Theory*, 38(11):1113–1131, 2003.

[11] A. Frisoli, D. Checcacci, F. Salsedo, and M. Bergamasco. *Advances in Robot Kinematics*, chapter Synthesis by screw algebra of translating in-parallel actuated mechanisms. Kluwer Academics, 2000.

[12] M. Carricato and V. Parenti-Castelli. A Family of 3-DOF Translational Parallel Manipulators. *Journal of Mechanical Design*, 125:302, 2003.